The hansenula polymorpha pex23 family: overlooked proteins In organelle formation

Wu, Fei

DOI:
10.33612/diss.157801525

CHAPTER 3

Structure function analysis of the ER-peroxisome contact site protein Pex32

Fei Wu, Arman Akşit, Arjen M. Krikken and Ida J. van der Klei

Molecular Cell Biology, Groningen Biomolecular Sciences and Biotechnology Institute, University of Groningen, 9300CC Groningen, The Netherlands

Abstract

Pex32 is an ER protein in the yeast *Hansenula polymorpha*, which is required for associating peroxisomes to the ER for controlling peroxisome abundance and size. Here, we report on a structure-function analysis of Pex32. By co-localization analysis of various Pex32 truncations, we demonstrated that the N-terminal transmembrane domain of Pex32 is responsible for sorting and function of the protein. The C-terminal DysF domain is required for concentrating Pex32 at ER-peroxisome contact sites and has the ability to bind to peroxisomes. Peroxisome defects in *pex32* cells might be caused by strongly decreased levels of Pex11. This is probably due to Pex11 degradation, because we were unable to obtain enhanced Pex11 levels in *pex32* cells upon *PEX11* overexpression. We previously showed that the peroxisomal membrane protein Pex11 is required for peroxisome-ER contact site formation as well as concentrating Pex32 at these sites. We now show that another peroxisomal membrane protein, Pex34, also affects Pex32 accumulation and ER-peroxisome associations. These data suggest that Pex32, Pex34 and Pex11 are involved in the same protein complex at ER-peroxisome contact sites. Overexpression of *PEX32* in *pex11* or *pex34* cells did not result in suppression of the peroxisome phenotypes indicating that Pex32, Pex11 and/or Pex34 are performing different roles in controlling peroxisome proliferation.

Introduction

Yeast peroxisomes are single membrane surrounded organelles, which adjust their abundance in response to the growth conditions (Smith and Aitchison, 2013). *PEX* genes encode peroxins that are involved in peroxisomal matrix protein import, membrane protein sorting and organelle proliferation. In yeast cells, both Pex11 family proteins and Pex23 family proteins are involved in controlling peroxisome proliferation (Yuan et al., 2016).

Most organisms contain multiple Pex11 family members, which almost all localize to the peroxisomal membrane. These include for instance Pex11, Pex25, Pex27 and Pex34 in *Saccharomyces cerevisiae* and Pex11, Pex25 and Pex11C in *Hansenula polymorpha*. Yeast Pex11 has been most extensively studied. It has an important role in peroxisome fission and functions in the initial peroxisome elongation step as well as in the final scission step (Farré et al., 2019). ScPex11 and ScPex34 also function at Peroxisome-Mitochondria (PerMit) contact sites (Mattiazzi Ušaj et al., 2015; Shai et al., 2018). These sites are important for efficient transport of β-oxidation products between both organelles (Shai et al., 2018). Deletion of Sc*PEX34* results in less peroxisomes per cell, but an increase in their size, like observed for *S. cerevisiae pex11* cells (Tower et al., 2011). The molecular mechanism of how ScPex34 controls peroxisome multiplication is still unknown. We recently showed that *H. polymorpha* Pex11 plays a role in peroxisome-ER contact sites. Whether Pex34 plays a role in contact sites other than PerMit is also not yet known.

Pex23 family proteins localize to the ER and only occur in fungi (Yuan et al., 2016). The number of Pex23 family members varies in different yeast species. The absence of Pex23

family members often results in abnormal peroxisome numbers and/or size (Yuan et al., 2016). So far, most studies focused on *S. cerevisiae* Pex30 to elucidate the role of Pex23 proteins in regulating peroxisome biogenesis. These studies suggested that ScPex30, together with its homologue ScPex29, and ER reticulons (Rtn1, Rtn2 and Yop1) form a protein complex at ER-peroxisome contact sites. This protein complex plays a role in regulating the formation of preperoxisomal vesicles (PPVs) from the ER by affecting ER curvature (Farré et al., 2019). We recently showed that in *H. polymorpha*, three Pex23 protein family members (Pex23, Pex24 and Pex32) play a role in the formation of ER-Peroxisome contact sites. Our data indicate that these sites are important for growth of the organellar membrane. In the absence of these peroxins, peroxisome biogenesis defects were observed that are accompanied by increased distances between the ER and peroxisome membranes. All these defects could be suppressed by the introduction of an artificial tethering protein that associates peroxisomes to the ER. Among these mutants, *H. polymorpha pex32* cells show the strongest peroxisome phenotypes. Protein sequence analysis resulted in the prediction of four transmembrane helices (TMs) in the N-terminus of Pex32 (Fig. 1A). This domain shows similarities with reticulon homology domain (RHD)-containing proteins. The C-terminus of Pex32 contains a DysF motif (Fig. 1A) (Wu et al., 2020). The function of DysF motif is not yet known.

In this study, we investigated structure-function relationships of Pex32. We show that the four predicted TMs in the N-terminal domain are sufficient for Pex32 function and sorting to the ER. The DysF domain is important for association of the protein with peroxisomes. Furthermore, we show that Pex34 has a similar function as Pex11 and is important for the formation of Pex32 containing peroxisome-ER contact sites. Pex11, Pex32 and Pex34 fulfil different functions, because overexpression of Pex32 does not suppress the phenotypes of *pex11* or *pex34* mutants. Intriguingly, in *pex32* cells Pex11 levels are strongly reduced, which cannot be restored by *PEX11* overexpression. This suggests that Pex32 is important for Pex11 sorting or stability.

Results

The Pex32 N-terminus localizes to the ER and the C-terminal DysF domain is cytosolic

Sequence analysis of *H. polymorpha* Pex32 resulted in the prediction of four transmembrane helices (TMs) in the N-terminus and a DysF motif at the C-terminus (Wu et al., 2020). Therefore most likely the extreme N- and C-terminus are oriented to the same side of the ER-membrane (Fig. 1A). To analyze which domains contain ER sorting information, we constructed several truncations containing GFP at the C-terminus. All truncations were introduced into the *pex32* strain. Considering the very low endogenous Pex32 levels, all truncated proteins were produced under the control of the strong P_{ADH1} promoter.

Using Confocal Laser Scanning Microscopy (CLSM Airy-scan), we observed that deletion of the DysF domain did not affect sorting to the ER (strain *pex32*::Pex32$^{TM(I\text{-}IV)}$, Fig. 1B). Similarly, removal of the extreme 31 N-terminal residues (*pex32*::Pex32$^{\Delta 31}$) resulted in a truncated protein that co-localized with the ER marker Bip-mCherry-HDEL. Hence, both the DysF domain and the extreme N-terminus are not essential for ER sorting of Pex32.

Next, we analyzed truncated species that lacked the DysF domain together with one or more TM domains. All constructs fully co-localized with the ER marker, except for the construct containing only TM(I), which partially localized to the cytosol as well (Fig. 1B). These data indicate that not all four TMs are necessary to sort a reporter to the ER. Moreover, our observation that constructs TM(III+IV) and TM(II) show an ER localization pattern, suggests that Pex32 contains redundant ER sorting information. Further analysis is required to reveal whether all four TMs contain sorting information for the ER.

A construct that consisted of only the DysF domain (without any predicted TM domain) localized predominantly to the cytosol. However, in addition some spots of higher fluorescence intensity could be detected (Fig. 1C). Because Pex32 accumulates at peroxisome-ER contacts, we subsequently asked whether these spots represent peroxisomes. Co-localization experiments using the peroxisomal membrane marker protein Pex14-mKate2 showed that, in glucose-grown cells, approximately half of the Pex32^{DysF}-GFP spots (partially) overlapped with Pex14-mKate2 spots (Fig. 1C), indicating that the DysF domain not only associates with peroxisomes but also with other, yet unknown structures.

We next performed a similar analysis of *pex32*::P_{ADH1}Pex32^{DsyF}-GFP cells grown at peroxisome inducing conditions (growth for 7 h on media containing methanol/glycerol), which results in an increase in peroxisome size and number. In these cells a ring of GFP fluorescence could be observed, that co-localized with the peroxisome marker Pex14-mKate2 (Fig. 1C). Together these data indicate that the DysF domain is capable to associate with peroxisomes.

Western blot analysis confirmed that all Pex32 variants were present at the expected

molecular weight. In cells of the *pex32*::Pex32$^{TM(I-III)}$, *pex32*::Pex32$^{\Delta 31}$, *pex32*::Pex32$^{TM(II-IV)}$ and *pex32*::Pex32$^{TM(III-IV)}$ strains, the protein levels were lower compared to that in the strain producing full length Pex32-GFP (Fig. 1D). Especially the level of construct TM(III-IV) was extremely low.

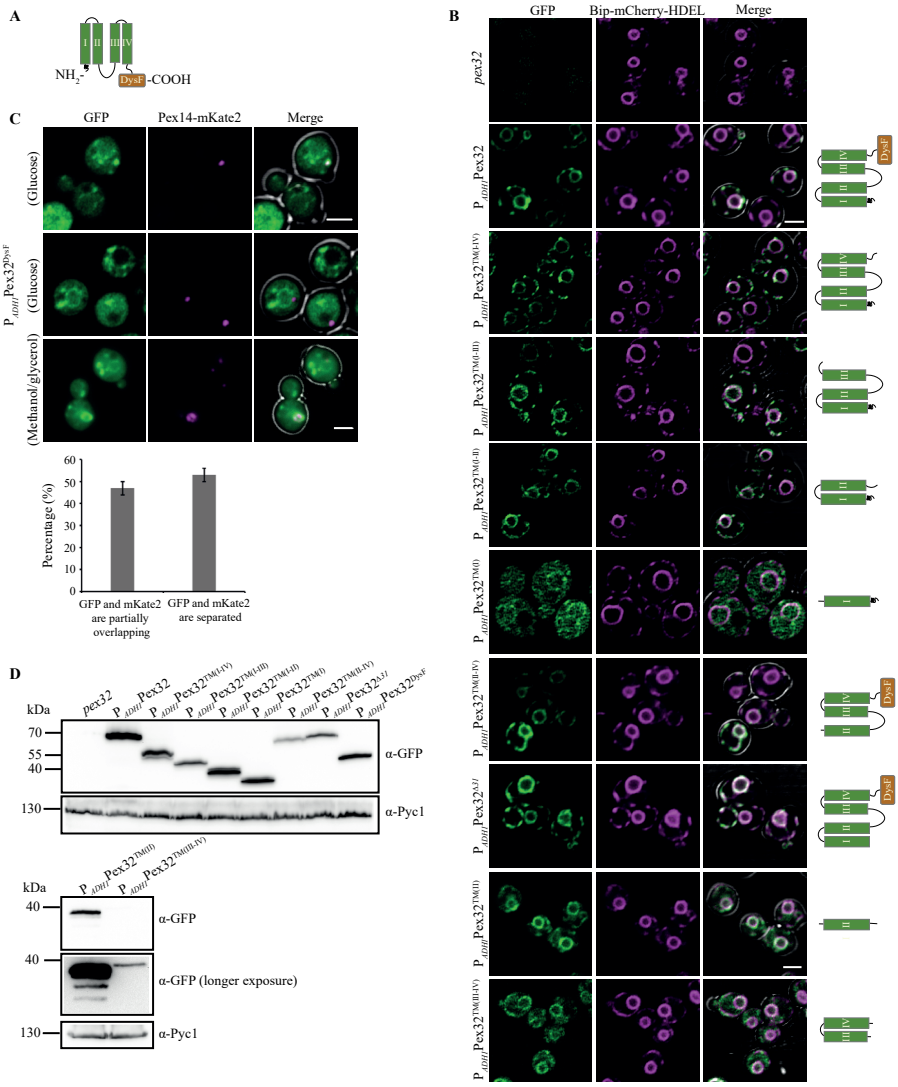

Figure 1. Pex32 TMs contain ER sorting information and the DysF domain can localizes to peroxisomes. (A) Predicted Pex32 structure. Transmembrane helixes (TMs) are numbered I, II, III and IV. (B) Confocal Laser Scanning Microscopy (CLSM) Airy-scan analysis of glucose-grown *pex32* cells producing Bip-mCherry-HDEL and the indicated Pex32 truncations fused to GFP and produced under control of the P_{ADH1}. Scale bars: 2 µm. (C) Top: CLSM Airy-scan images of

glucose-grown cells and fluorescence microscopy (FM) images of methanol/glycerol-grown *pex32* cells producing Pex14-mKate2 and P_{ADH1}Pex32^{DysF}-mGFP. Bottom: quantification of percentage of GFP spots partially overlapping with mKate2 spots in glucose-grown cells. The error bars represent s.d. from two independent experiments (n=2 using 30 cells for the quantification of colocalization). Scale bars: 2 μm (D) Western blot analysis of the indicated strains grown on glucose for 4 h. Blots were decorated with anti-GFP or anti-Pyc1 antibodies. Pyc1 was used as a loading control.

The DysF domain is not essential for Pex32 function in peroxisome biogenesis

To analyze the importance of the different domains of Pex32 for its function in peroxisome biogenesis, we checked peroxisome abundance and function in *pex32* strains producing various Pex32 truncations containing GFP at the C-terminus. To rule out effects of protein overproduction, all truncations were produced under control of the endogenous promoter (P_{PEX32}). A WT strain producing full length Pex32 (Pex32^{FL}-GFP) under control of its own promoter was used as control. FM analysis revealed that relative to *pex32* cells peroxisome numbers only increased to WT levels upon introduction of a construct that contains the intact N-terminus (*pex32*::Pex32$^{TM(I-IV)}$) (Fig. 2A). In all other strains only a slight increase in peroxisome number could be observed (Fig. 2B). In line with these observations, the growth defect of *pex32* cells on medium containing a mixture of glycerol and methanol was fully rescued upon production of the entire Pex32 N-terminus (*pex32*::Pex32$^{TM(I-IV)}$), while growth of all other strains only slightly improved (Fig. 2C). These findings indicate that the complete N-terminus, but not the DysF domain, is essential for Pex32 function.

Western blotting was performed to check whether all constructions were produced and of the expected size. As shown in Fig. 2D, except for the protein levels of Pex32$^{TM(II-IV)}$ and Pex32$^{\Delta 31}$ which were below the limit of detection, all other truncations were detectable and present at the expected size (Fig. 2D). However, for full length Pex32, as well as for some of the truncations also a band of approx. 27 kDa was present, which most likely represents free GFP. The observation that Pex32$^{TM(II-IV)}$ or Pex32$^{\Delta 31}$ could not suppress the phenotype of *pex32* cells, could be related to the very low protein amounts (Fig. 2D). All these data imply that a minimum amount of Pex32 TMs is important to ensure the function of Pex32 in controlling peroxisome abundance.

We previously showed that in glucose-grown cells Pex32-GFP, produced under control of the endogenous promoter (P_{PEX32}), accumulates in a single spot, which represents the peroxisome-ER contact site. However, upon removal of the DysF domain, instead multiple fainter GFP spots were observed (in *pex32*::Pex32$^{TM(I-IV)}$ cells) (Fig. 2E). This means that the DysF domain of Pex32 is required for keeping the protein at peroxisome-ER contacts.

Taken together, we conclude that in *H. polymorpha* Pex32, the DysF motif is involved in Pex32 accumulation at peroxisome-ER contacts, while the N-terminus containing the four transmembrane regions is crucial for its function in peroxisome biogenesis.

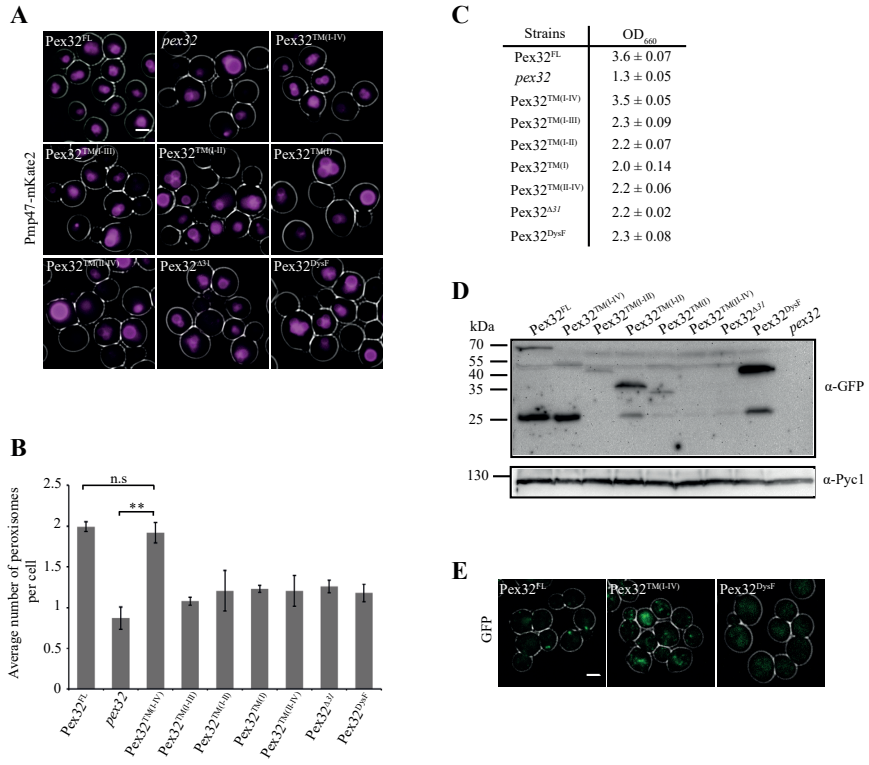

Figure 2. The N-terminal domain of Pex32 is important for its function, while the DysF domain is required to accumulate Pex32 at peroxisome-ER contact sites. (A) FM analysis of methanol/glycerol grown *pex32* cells producing Pmp47-mKate2 and the indicated Pex32 truncations containing GFP at the C-terminus and produced under control of the P_{PEX32}. Scale bar: 2 µm. (B) Quantification of the average number of peroxisomes per cell in the indicated strains. The error bars represent s.d. from three independent experiments (n=3 using 200 cells from each experiment). Significance indications: n.s = $p > 0.05$, ** = $p < 0.01$. (C) Optical densities of the indicated strains upon growth for 16 h on methanol/glycerol medium. Average values (± SD) are shown from three independent cultures. (D) Western blot analysis of the indicated strains. Cells were grown on methanol/glycerol medium for 16 h. Blots were decorated with anti-GFP or anti-Pyc1 antibodies. Pyc1 was used as a loading control. (E) FM analysis of glucose-grown WT cells producing Pex32-GFP or *pex32* cells producing $Pex32^{TM(I-IV)}$ and $Pex32^{DysF}$. Scale bar: 2 µm.

The reduction of peroxisome abundance in *pex32* cells is not caused by enhanced autophagy

Deletion of *PEX32* results in a strong reduction of peroxisome numbers (Wu et al., 2020). In order to test whether this is due to enhanced organelle degradation by autophagy, *ATG1*, which is known to be essential for autophagy, was deleted in *pex32* cells (Komduur et al., 2003). FM analysis of cells producing the matrix marker DsRed-SKL revealed that the

decrease in peroxisome numbers relative to WT controls was similar in *pex32* and *pex32 atg1* cells (Fig. 3A,B). Hence, autophagy is not responsible for the decreased peroxisome numbers.

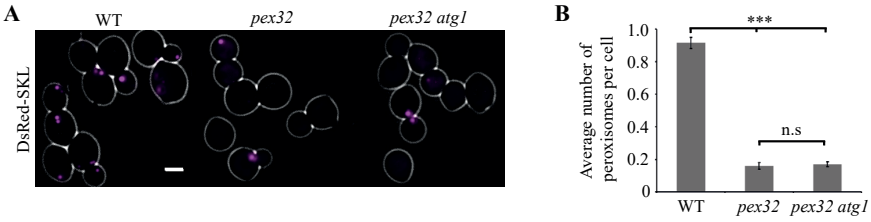

Figure 3. Pexophagy is not enhanced in *pex32* cells. (A) FM images of DsRed-SKL produced in WT, *pex32* and *pex32 atg1* cells grown on glucose for 4 h. Scale bar: 2 μm. (B) Quantification of the average number of peroxisome per cell in the indicated strains. The error bars represent s.d. from three independent experiments (n=3 using 200 cells from each experiment). Significance indications: n.s = $p > 0.05$, *** = $p < 0.001$.

Deletion of *PEX32* results in reduced Pex11 levels

Next, we compared the levels of several peroxisomal proteins in *pex32* and WT control cells to find out whether the peroxisome biogenesis defects in *pex32* cells are accompanied by changes in the levels of other peroxins. Because *pex32* cells are unable to grow in methanol medium, we used medium containing a mixture of methanol and glycerol to induce peroxisomal proteins (Wu et al., 2020). As shown in Fig. 4A, the levels of the peroxisomal membrane proteins (PMPs) Pex3 and Pex14, and the peroxisomal matrix protein alcohol oxidase (AOX) were similar in *pex32* and WT cells. However, the level of Pex11 was strongly reduced in *pex32* cells (Fig. 4A,B).

This prompted us to investigate whether the phenotype of *pex32* cells could be restored by *PEX11* overexpression using the strong *AOX* promoter (P_{AOX}). The peroxisomal matrix protein GFP-SKL was used to mark peroxisomes. FM images of cells grown for 6 hours on methanol/glycerol revealed that *PEX11* overexpression resulted in enhanced peroxisome proliferation in WT and *pex11* controls, as expected (Fig. 4C). In contrast, both *pex32* and *pex32*::P_{AOX}Pex11 cells showed mislocalization of GFP-SKL to the cytosol, indicating that peroxisome biogenesis was still severely affected upon Pex11 overproduction (Fig. 4C). Western blot analysis confirmed the strong increase in Pex11 protein levels in WT and *pex11* cells upon Pex11 overproduction. However, unexpectedly, we found that Pex11 levels were not enhanced in cells of the *pex32* deletion strain upon introduction of P_{AOX}Pex11.

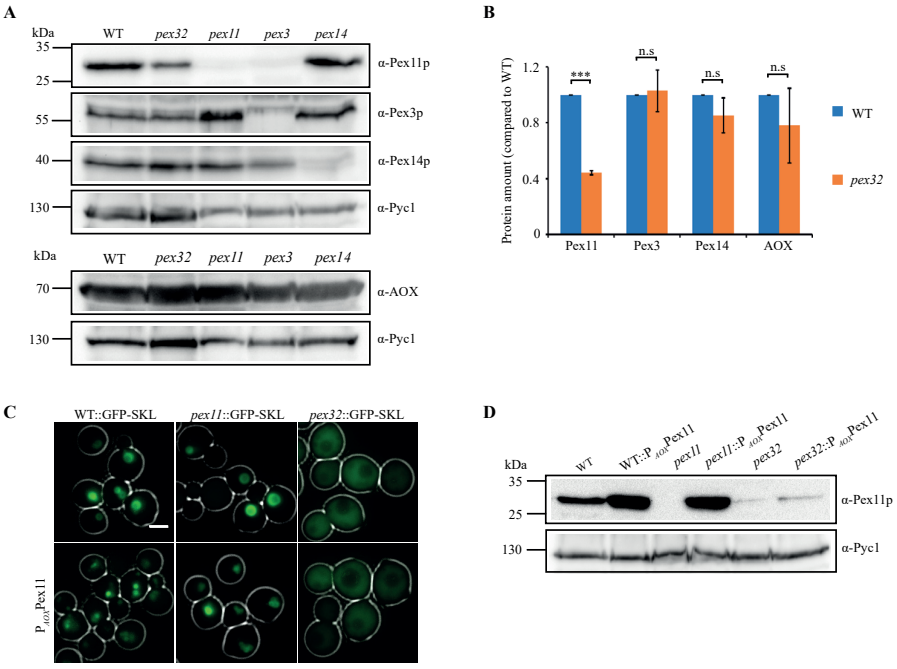

Figure 4. Protein levels of Pex11 decrease in *pex32* mutants. (A) Western blot analysis and (B) quantification of the indicated proteins in WT, *pex32* and indicated negative control cells grown for 16 h on methanol/glycerol. Blots were decorated with anti-Pex11p, anti-Pex3p, anti-Pex14p, anti-AOX or anti-Pyc1 antibodies. Pyc1 was used as a loading control. In B, the protein levels of WT cells were set to 1. Significance indications: n.s = $p > 0.05$, *** $p = 0.0007 < 0.001$. The error bars represent s.d. from three independent experiments. (C) FM images of WT, *pex11* and *pex32* cells producing GFP-SKL grown on methanol/glycerol for 6 h. Scale bar: 2 µm. (D) Western blot analysis of the indicated strains grown on methanol/glycerol for 6 h. Blots were decorated with anti-Pex11p or anti-Pyc1 antibodies. Pyc1 was used as a loading control.

Pex34 is required for the formation of ER-peroxisome contact sites

S. cerevisiae Pex34 functions together with Pex11 family proteins in regulating peroxisome abundance (Tower et al., 2011). The same proteins were shown to be involved in peroxisome-mitochondria contact sites (Shai et al., 2018). In *H. polymorpha* Pex11 plays a role in peroxisome-ER contacts. Hence, these proteins function in multiple peroxisomal membrane contacts. In order to study whether *H. polymorpha* Pex34 is also involved in peroxisome-ER contacts, we first identified the putative *H. polymorpha* Pex34 homologue of *S. cerevisiae* Pex34. Multiple Sequence Alignment (MSA) of the putative *H. polymorpha* Pex34 with various yeast Pex34 proteins revealed regions that are highly conserved. However, very little sequence homology is observed at the N-terminus (Fig. 5).

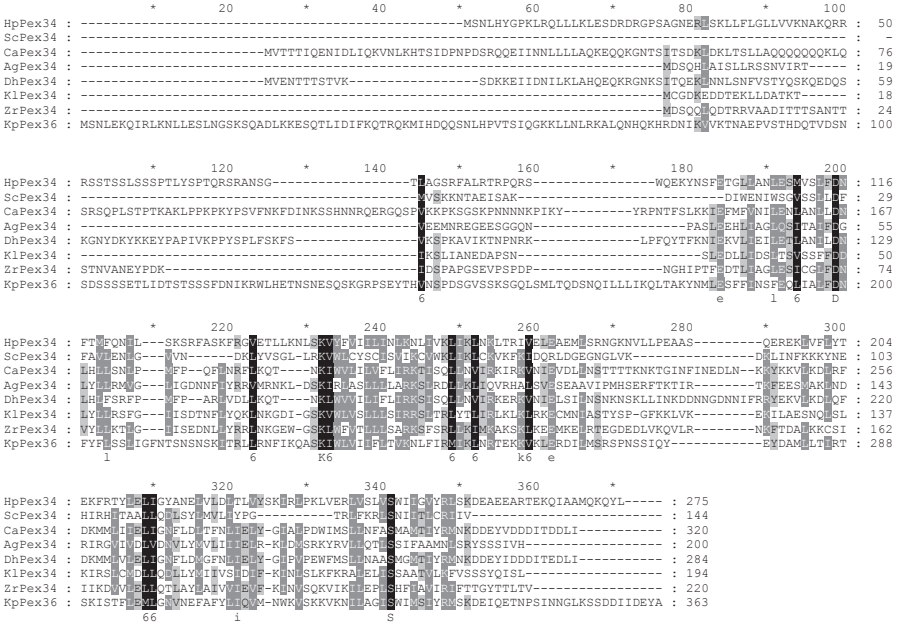

Figure 5. Sequence alignment of yeast Pex34 proteins. The sequences were first aligned using the CLUSTAL-X program and visualized by the GeneDoc program. Gaps were introduced to maximize the similarity. Colors were assigned to indicate strongly conserved positions in a decreasing order of conservation: "black", "dark gray" and "light gray". "6" below black residues indicates the presence of a non-polar amino acid. Capital letters indicate the conserved residues. Small letters below the gray residues indicate the most conserved amino acid among the sequences. Ca - *Candida albicans* KGU18165; Dh - *Debaryomyces hansenii* CAG88545; Zr - *Zygosaccharomyces rouxii* CAR29068; Kl - *Kluyveromyces lactis* CAH01071; Ag - *Ashbya gossypii* AAS54114; Kp - *Pichia pastoris* (*Komagataella phaffii*) CAY67701; Hp - *H. polymorpha* OBA14840; Sc - *Saccharomyces cerevisiae* CAA99168. Asterisks and numbers mark amino acids positions in the alignment. The ScPex34 homolog of *P. pastoris* is named Pex36 (Farré et al., 2017).

Co-localization analysis of a strain producing both Pex34-GFP and DsRed-SKL, confirmed that the identified protein is peroxisomal (Fig. 6A). Analysis of a constructed *PEX34* deletion strain showed that peroxisome numbers were reduced, concomitant with a growth defect on methanol medium (Fig. 6B,C,D). Importantly, this phenotype resembles that of *H. polymorpha pex11* or *pex32* cells (Krikken et al., 2009; Wu et al., 2020).

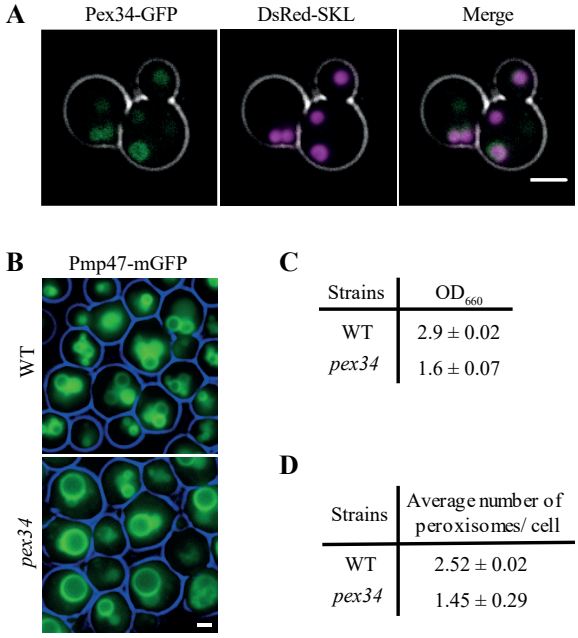

Figure 6. Pex34 localizes to peroxisomes and is important for normal peroxisome abundance and methanol growth. (A) FM analysis of *H. polymorpha* WT cells producing both GFP fused Pex34 C-terminally and the peroxisome matrix protein DsRed-SKL. Cells were grown on mineral medium containing methanol for 6 hours. Scale bar: 2 µm. (B) FM analysis of WT and the *pex34* deletion strain producing the peroxisomal membrane marker PMP47-GFP. Cells were grown for 16 hours on mineral medium containing methanol. Scale bar: 1 µm. (C) Optical densities of the indicated cultures upon growth for 16 h on methanol. Average values (± SD) are shown from two independent cultures. (D) Quantification of the average peroxisome numbers in methanol grown cells. Average values (± SD) are shown from two independent cultures. 2 x 500 peroxisomes from two independent cultures were quantified.

We previously showed that Pex32 is an ER protein that accumulates in spots at peroxisome-ER contacts, a pattern that disappeared in *pex11* cells (Wu et al., 2020; Fig. 7A). FM analysis showed that also in *pex34* cells producing Pex32-GFP, GFP fluorescence are present in multiple faint spots, which are spread over the cell and not always close to the peroxisomal marker Pex14-mKate2 (Fig. 7A). This is not due to lower protein levels, as Pex32-GFP protein levels are similar in WT and *pex34* cells (Fig. 7B).

In *H. polymorpha* WT cells, close associations (< 10 nm) between the ER and peroxisome are observed (Wu et al., 2018), which are lost in the absence of Pex32 or Pex11 (Wu et al., 2020). Similar as in *pex11* cells (Wu et al., 2020) only 30% of the peroxisomes occur at a distance of < 10 nm from the ER in *pex34* cells, while this is over 80% in WT controls (Fig. 7C) (Wu et al., 2020). These data show that deletion of *PEX34* or *PEX11* results in defects in peroxisome-ER contact sites and an altered Pex32 localization pattern.

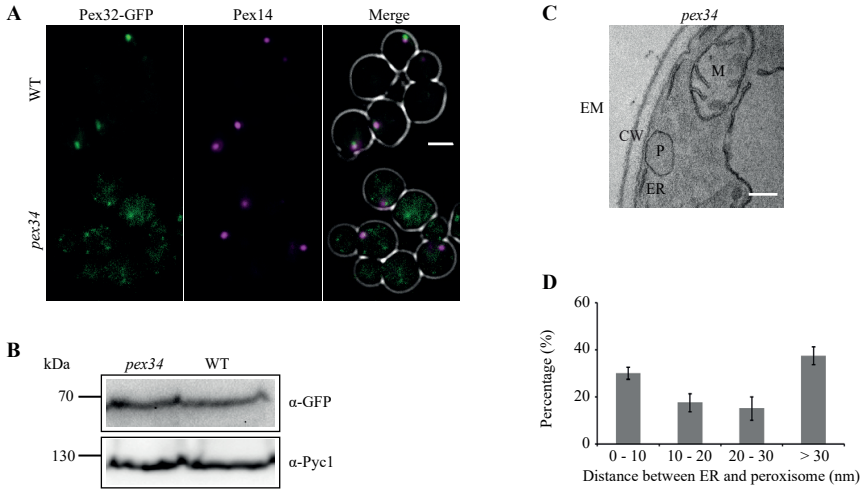

Figure 7. Deletion of *PEX34* has an effect on Pex32 localization and results in a distance increase between peroxisome and the ER membrane. (A) FM images of glucose-grown *pex34* mutant cells producing Pex32-GFP under control of its endogenous promoter together with the peroxisomal marker Pex14-mKate2. Scale bar: 2 µm. (B) Western blot analysis of the indicated strains. Blots were decorated with anti-GFP or anti-Pyc1 antibodies. Pyc1 was used as a loading control. A representative blot of two experiments is shown (C) EM image of $KMnO_4$-fixed glucose-grown *pex34* mutant cell. CW - cell wall; ER - endoplasmic reticulum; P - peroxisome; M - mitochondrion. Scale bar: 200 nm. (D) Quantification of the distance between peroxisome and ER membranes in *pex34* cells grown on glucose. The error bars represent s.d. from two independent experiments (n=2 using 20 cell sections from each experiment).

Overexpression of Pex32 does not suppress peroxisome defects in *pex34* or *pex11* cells

To investigate whether Pex32 is functionally redundant with Pex11 or Pex34, we overproduced Pex32-GFP in *pex11* and *pex34* strains by placing the gene under control of the strong P_{ADH1} promoter. Western blot analysis confirmed that the protein was overproduced in all strains (Fig. 8B). Notably, upon overproduction a clear second band around 27 kDa was evident, which probably represent the free GFP. FM analysis revealed that overproduced Pex32-GFP shows the typical cortical/nuclear ER pattern in all strains (WT, *pex11*, *pex34* and *pex32*) (Fig. 8A).

Next, we quantified peroxisome numbers in all above mentioned strains. As shown in Fig. 8C, overexpression of *PEX32* restored peroxisome numbers in *pex32* cells to numbers similar as in WT controls. No significant increase in peroxisome number could be observed in any of the other strains upon overexpression of *PEX32* (Fig. 8C). In line with this observation, only the growth defect of *pex32* cells on methanol medium was restored by overproducing *PEX32*, but not that of the *pex11* or *pex34* deletion strains (Fig. 8D).

Based on these data we conclude that overexpression of *PEX32* does not suppress the phenotypes of *pex11* or *pex34* deletion strains, which means that there is no functional redundancy.

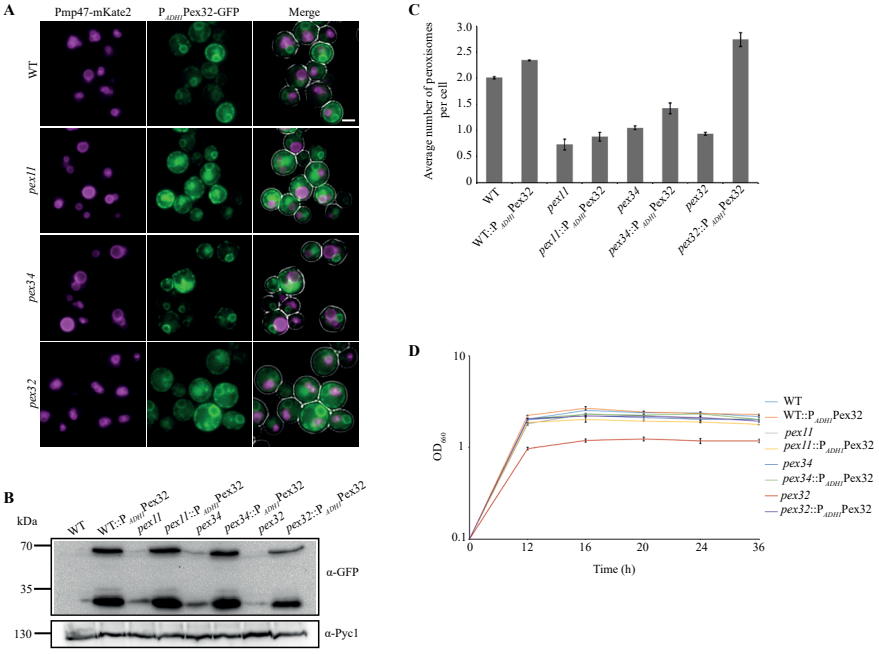

Figure 8. Overexpression of *PEX32* does not result in suppression of the peroxisomal phenotypes of *pex11* and *pex34* cells. (A) FM images of the indicated strains producing P_{ADH1}Pex32-mGFP, grown on methanol/glycerol for 16 h. Scale bar: 2 µm. (B) Western blot analysis of the indicated strains grown on methanol/glycerol for 16 h. Blots were decorated with anti-GFP or anti-Pyc1 antibodies. Pyc1 was used as a loading control. A representative blot of two blots (biological replicate) is shown. (C) Quantification of the average peroxisome number per cell in the indicated strains. The error bars represent s.d. from two independent experiments (n=2 using 200 cells from each experiment). (D) Growth curve of the indicated strains in medium containing a mixture of methanol and glycerol. The cell density is indicated as optical density at 660 nm (OD_{660}). The error bars represent s.d. from two independent cell cultures.

Discussion

In this study, we show that both the sorting and the function of Pex32 depend on its TMs, while the DysF domain plays a role in concentrating Pex32 at peroxisome-ER contact sites. In addition, our data reveal that not only Pex11 but also Pex34 is important for the formation of Pex32-dependent peroxisome-ER contact sites. The roles of these three proteins in regulating peroxisome abundance and size differ.

Using various truncated Pex32 variants, we studied which region in the N-terminal,

membrane bound part of Pex32 contains ER sorting information. For the *S. cerevisiae* Pex23 family proteins Pex30 and Pex31, it was shown that this region contains a reticulon-homology domain (RHD), which is required for localizing proteins at curved regions of the ER such as tubular ER and the edge of ER sheets (Joshi et al., 2016). We previous reported that a RHD also exists in *H. polymorpha* Pex32 although the prediction was borderline (Wu et al., 2020).

Possibly, Pex32 uses a similar protein insertion mechanism as other ER localized RHD-containing proteins. *In vitro* transcription and immunoprecipitation assays revealed that human reticulons could be either co-translationally inserted into the ER membrane or guided by Pex19 through a post-translational route (He et al., 2007; Yamamoto and Sakisaka 2018). It has also been proposed that the structural features of TMs, rather than a specific amino acid sequence, might be responsible for reticulon targeting, as no recognizable signal peptide could be found in known reticulons (Yan et al., 2006). Similarly, we were unable to find a signal peptide in *H. polymorpha* Pex32. We found that all truncations that contain TM(II) show a clear ER localization pattern. In comparison, in cells producing only TM(I) or TM(III-IV), in which the second TM is missing, some cytosolic GFP signal could be observed as well. This indicates that TM(II) of Pex32 is important for sorting a reporter to the proper position of the ER.

In addition to Pex32, *H. polymorpha* has three additional Pex23 family proteins, Pex23, Pex24 and Pex29. These proteins all localize to the ER (Wu et al., 2020). Possibly these Pex32 homologues may interact with TM(II) of Pex32 and help to insert it into the ER membrane.

Western blot analysis reveals that deletion of the first 31 N-terminal residues before TM(I) causes a very strong decrease in protein levels. Possibly, the absence of this part makes this protein more susceptible to proteolytic degradation.

Based on our data it is clear that the entire N-terminus, but not the DysF motif, is essential for the role of Pex32 in controlling peroxisome abundance and size, based on the finding that peroxisome deficiencies are completely restored in *pex32*::Pex32$^{TM(I-IV)}$ cells. This is different from previous findings in other yeast species, which showed that the DysF domain of *P. pastoris* Pex30 and Pex31 are essential for peroxisome number and size regulation (Yan et al., 2008). Instead, we found that the accumulation of HpPex32-GFP at peroxisome-ER contact sites requires the DysF motif, because the GFP signal was no longer present in one or a few spots when the DysF motif was missing. Moreover, our data also indicate that the Pex32 DysF domain has the ability to associate to peroxisomes. Interestingly, we previously showed that most *pex32* cells have no peroxisomes (Wu et al., 2020). However, multiple GFP spots could be observed per cell in *pex32*::P_{ADHI}Pex32^{DysF}-GFP cells, which suggests that the DysF motif could associate not only to peroxisomes but also to other structures.

Pex32 has two RWL tripeptides in its DysF domain. An R-W-L motif also exists in the transmembrane domain of ScSey1 (Synthetic enhancer of Yop1 protein) and has the ability

to bind sterols (Lee et al., 2019). Possibly, the DysF-GFP spots that do not co-localize with Pex14-mKate2, represent sterol-containing structures. This could also explain the slight increase in peroxisome numbers in *pex32*::Pex32^{DysF} cells, in which the DysF domain may help to bring sterols to the peroxisomal membrane for organellar growth.

As expected, *pex32*::Pex32$^{TM(I-IV)}$ cells can grow on methanol/glycerol like WT cells because of the defects in peroxisome formation are suppressed. In addition, all other truncations that show a slight growth improvement relative to the *pex32* deletion strain also have a minor increase in average peroxisome numbers. Because all Pex32 N-terminal truncations are sorted on the ER, it is possible that the reintroduced Pex32 N-terminal truncations have an effect on the ER, which stimulates peroxisome formation. The low protein levels of these truncations may explain why the peroxisome deficiency is not rescued completely.

Similar to the described characteristics of *S. cerevisiae* Pex34 (Tower et al., 2011), our data demonstrate that *H. polymorpha* Pex34 is a peroxisome membrane protein involved in the regulation of peroxisome number and size. Interestingly, in *pex34* cells we observed a change in Pex32 localization pattern and an increased ER-peroxisome distance, indicating that Pex34 is required for the formation of Pex32-dependent ER-peroxisome contacts. In fact, these results are similar to our previous findings in *pex11* cells (Wu et al., 2020), which highly suggests that Pex11 and Pex34 might be Pex32 interaction proteins in maintaining the association between the ER and peroxisome. Actually, both ScPex34 and ScPex11 are peroxisome-mitochondria (PerMit) contact sites tethers (Shai et al., 2018). Because we only analyzed the interaction between ER and peroxisome membrane proteins, it is possible that HpPex34 and HpPex11 are also involved in multiple peroxisome contact sites by interacting with different organellar membrane proteins.

Apart from the defects in ER-peroxisome contacts, we found that cells lacking Pex32 have strongly reduced Pex11 levels, while the levels of other PMPs were normal. Moreover, upon placing *PEX11* under control of a strong promoter, Pex11 protein levels were not enhanced. Pex11 is an important peroxisome membrane protein and plays a crucial role in regulating peroxisome membrane elongation as well as peroxisome scission during peroxisome fission (Farré et al., 2019). In the absence of *PEX32*, Pex11 levels are insufficient to facilitate normal peroxisome proliferation by fission, indirectly leading to enlarged organelles in the *pex32* deletion strain.

Besides the role in organelle fission, Pex11 could also affect Pex32-dependent peroxisome biogenesis by affecting the lipid composition of peroxisomal membranes. Pex11 has been identified as a peroxisome-mitochondrion contact site protein and interacts with ER-Mitochondria Encounter Structure (ERMES) components in *S. cerevisiae* (Farré et al., 2019; Shai et al., 2018; Mattiazzi Ušaj et al., 2015). ERMES proteins, except for Mdm10, all contain an SMP (Synaptotagmin-like Mitochondrial lipid-binding Proteins) domain that has the ability to bind lipids and could contribute to lipid transfer between the ER and mitochondria (Kopec et al., 2010). If a similar functional protein complex exists in *H.*

polymorpha, it is possible that Pex11 is responsible for transferring lipids from the ER and/or mitochondria to peroxisomes by interacting with ERMES components. The reduced Pex11 levels would affect the process of lipids uptake and further result in peroxisome biogenesis defects. Moreover, Pex11 has also been found to be involved in lipid homeostasis in *Y. lipolytica* (Dulermo et al., 2015), which suggests there is a relationship between Pex11 and organellar lipid composition.

Finally, as expected, overexpression of *PEX32* suppressed the peroxisomal phenotypes in *pex32* cells. In fact, the average peroxisomes numbers were even somewhat higher than in WT controls. Moreover, all cells (WT control, *pex11* and *pex34* mutations) show a minor peroxisome number increase when Pex32 is overproduced. As Pex32 is an ER protein and has four TMDs, we cannot rule out that the shape of the ER is changed upon overexpression of *PEX32*, which could indirectly benefit organelle proliferation. However, the peroxisome numbers were still lower in *pex11*::P_{ADH1}Pex32 and *pex34*::P_{ADH1}Pex32 cells compared to WT controls and showed no significant difference with the single deletion strains. Hence, the peroxisome membrane proteins Pex11 and Pex34 are still mainly responsible for controlling organelle growth and division.

Summarizing, our data indicates that the membrane bound domain of Pex32 is important for its function at the ER, while the DysF domain is important to concentrate Pex32 at the ER region where peroxisomes closely associate with the ER. The peroxisomal membrane proteins Pex11 and Pex34 are also important for the formation of peroxisome-ER contact sites and to keep Pex32 concentrated at these spots. Therefore, they are likely candidates to interact with Pex32 at EPCONs.

Materials and methods

Strains and growth conditions

H. polymorpha cells were grown in batch cultures at 37 °C on mineral media (Van Dijken et al., 1976) supplemented with 0.5% glucose, 0.5% methanol, 0.25 % glycerol or a mixture of 0.5% methanol and 0.05% glycerol as carbon source. Leucine, when required, was added to a final concentration of 60 μg/ml. For growth on plates, YPD media (1% yeast extract, 1% peptone and 1% glucose) or YND media (0.67% yeast nitrogen base without amino acids (YNB; Difco; BD) and 0.5% glucose) were supplemented with 2% agar. Resistant transformants were selected using 100 μg/ml zeocin (Invitrogen), or 100 μg/ml nourseothricin (WERNER BioAgents) or 300 μg/ml hygromycin (Invitrogen).

The *Escherichia coli* strain DH5α was used for cloning. *E. coli* cells were grown at 37 °C in Luria broth (LB) media (1% Bactotryptone, 0.5% Yeast Extract and 0.5% NaCl) supplemented with 100 μg/ml Ampicillin or 50 μg/ml kanamycin. 2% agar was added in LB medium when growing on plates.

Construction of *H. polymorpha* strains

The strains, plasmids and primers used in this study are listed in Table 1, 2 and 3, respectively. Plasmid integration was performed as described previously (Faber et al., 1994). All integrations were confirmed by PCR. Gene deletions were confirmed by PCR and southern blotting.

Construction of strains expressing GFP tagged Pex32 truncations

Plasmids encoding P_{ADH1}Pex32$^{TM(I-IV)}$-mGFP and P_{ADH1}Pex32^{DysF}-mGFP were constructed as follows: a PCR fragment encoding the N-terminus (all four transmembrane helices) of *PEX32* was obtained using primers Fw Pex32$_{1-696}$ and Rv Pex32$_{1-696}$ with *H. polymorpha yku80* genomic DNA as a template. Similarly, a PCR fragment encoding the DysF domain of *PEX32* was obtained with primers Fw Pex32$_{697-1062}$ and Rv Pex32$_{697-1062}$. The obtained PCR fragments were digested with *Hin*dIII and *Bgl*II, and separately inserted between the *Hin*dIII and *Bgl*II sites of plasmid pHIPZ18-*INP1*-GFP, resulting in pHIPZ18-*PEX32*$^{TM(I-IV)}$-mGFP and pHIPZ18-*PEX32*^{DysF}-mGFP. Both plasmids and pAMK106 were restricted by *Hin*dIII and *Sal*I, fragments ligation to get plasmids pHIPN18-*PEX32*$^{TM(I-IV)}$-mGFP and pHIPN18-*PEX32*^{DysF}-mGFP.

By using pHIPN18-*PEX32*$^{TM(I-IV)}$-mGFP as the template, primer pairs: i) Fw Pex32$_{1-696}$/ Rev Pex32$_{1-501}$, ii) Fw Pex32$_{1-696}$/Rev Pex32$_{1-312}$, and iii) Fw Pex32$_{1-696}$/Rev Pex32$_{1-177}$ were used to amplify constructs containing: i) *PEX32*$^{TM(I-III)}$, ii) *PEX32*$^{TM(I-II)}$, and iii) *PEX32*$^{TM(I)}$ respectively. PCR products were digested with *Hin*dIII and *Bgl*II, and inserted between the *Hin*dIII and *Bgl*II sites of pHIPN18-*PEX32*$^{TM(I-IV)}$-mGFP separately to obtain pHIPN18-*PEX32*$^{TM(I-III)}$-mGFP, pHIPN18-*PEX32*$^{TM(I-II)}$-mGFP and pHIPN18-*PEX32*$^{TM(I)}$-mGFP.

Plasmids pHIPN18-*PEX32*$^{TM(II-IV)}$-mGFP and pHIPN18-*PEX32*$^{\Delta 31}$-mGFP were constructed by using the same method: *H. polymorpha* Pex32-mGFP cells were used as the template, using primer pairs Fw Pex32$_{(169-1062)}$/Rv DysF$_{PEX32\text{-}mGFP}$ and Fw Pex32$_{(94-1062)}$/ Rv DysF$_{PEX32\text{-}mGFP}$ to amplify fragments containing *PEX32*$^{TM(II-IV)}$-mGFP and *PEX32*$^{\Delta 31}$-mGFP respectively. Both PCR products and pHIPN18-*PEX32*$^{TM(I-IV)}$-GFP were restricted by *Hin*dIII and *Xho*I separately, resulting in pHIPN18-*PEX32*$^{TM(II-IV)}$-mGFP and pHIPN18-*PEX32*$^{\Delta 31}$-mGFP.

The plasmid for *PEX32* overexpression was constructed as follows: a PCR fragment containing full-length *PEX32* was obtained using primers Fw Pex32$_{1-696}$ and Rv DysF$_{PEX32\text{-}mGFP}$ with Pex32-mGFP strain as a template. The PCR product and pHIPN18-Pex32$^{TM(I-IV)}$-mGFP were digested by *Hin*dIII and *Xho*I, ligated resulting in pHIPN18-*PEX32*-mGFP.

All above plasmids were linearized with *Aat*II and integrated into *pex32* strains separately to produce P_{ADH1}Pex32-mGFP, P_{ADH1}Pex32$^{TM(I-IV)}$-mGFP, P_{ADH1}Pex32$^{TM(I-III)}$-mGFP, P_{ADH1}Pex32$^{TM(I-II)}$-mGFP, P_{ADH1}Pex32$^{TM(I)}$-mGFP, P_{ADH1}Pex32$^{TM(II-IV)}$-mGFP, P_{ADH1}Pex32$^{\Delta 31}$-mGFP or P_{ADH1}Pex32^{DysF}-mGFP. *Dra*I-linearized pHIPX7-Bip$_{N30}$-mCherry-HDEL was integrated into various truncations independently to express BiP-mCherry-HDEL.

To obtain pHIPN18-*PEX32*$^{TM(II)}$-mGFP and pHIPN18-*PEX32*$^{TM(III-IV)}$-mGFP, plasmid

pHIPN18-*PEX32*$^{TM(I-IV)}$-mGFP was used as a template, and primer pairs Fw Pex32$_{o2TM}$/ Rev Pex32$_{1-312}$, Fw Pex32$_{TM3+4}$/Rv Pex32$_{1-696}$ were used to amplify fragments containing *PEX32*$^{TM(II)}$ and *PEX32*$^{TM(II-IV)}$ respectively. These PCR products and pHIPN18-*PEX32*$^{TM(I-IV)}$-mGFP were digested with *Hin*dIII and *Bgl*II and ligated to ontain pHIPN18-*PEX32*$^{TM(II)}$-mGFP and pHIPN18-*PEX32*$^{TM(III-IV)}$-mGFP. *Aat*II-linearized plasmids were integrated into *pex32*::BiP-mCherry-HDEL separately to produce P_{ADH1}Pex32$^{TM(II)}$-mGFP and P_{ADH1}Pex32$^{TM(III-IV)}$-mGFP.

Plasmids for producing various Pex32 truncations under control of the *PEX32* promoter were constructed as follows: PCR was performed on *yku80* genomic DNA to amplify the *PEX32* promoter using primers P_{PEX32} fw and P_{PEX32} rev. The obtained PCR fragment was digested with *Not*I and *Hin*dIII, and then replaced the *ADH1* promoter (P_{ADH1}) in *Not*I/ *Hin*dIII digested variants of Pex32 truncations. All constructions under control of P_{PEX32} were linearized with *Eco*RV and integrated into *pex32*::Pmp47-mKate2 cells separately to produce Pex32$^{TM(I-IV)}$-mGFP, Pex32$^{TM(I-III)}$-mGFP, Pex32$^{TM(I-II)}$-mGFP, Pex32$^{TM(I)}$-mGFP, Pex32$^{TM(II-IV)}$-mGFP, Pex32$^{\Delta 31}$-mGFP and Pex32^{DysF}-mGFP.

Construction of the *pex32 atg1* double deletion strain and the *pex34* deletion strain

To construct *pex32 atg1*, a PCR fragment containing the *ATG1* deletion cassette was amplified with primers pDEL-ATG1-fwd and pDEL-ATG1-rev using plasmid pARM011 as a template. The resulting *ATG1* deletion cassette was transformed into *pex32* cells to get double mutant of *pex32 atg1*. *Dra*I-linearized pAMK15 plasmid was transformed into *pex32 atg1* cells to produce DsRed-SKL.

The *pex34* deletion strain was constructed by replacing the *PEX34* region with the hygromycin resistance gene as follows: first, two PCR fragments comprising the *PEX34* flanking regions were amplified with primer pairs pex34-1/pex34-2 and pex34-3/pex34-4 using WT genomic DNA as the template. The PCR fragments were cloned into the vectors pDONR P4-P1R and pDONR P2R-P3, respectively, resulting in the entry vectors pENTR-*PEX34* 5' and pENTR-*PEX34* 3'. Recombination of these two entry vectors together with pENTR221-hph and the destination vector pDEST-R4-R3, resulting in pAMK57. Using pAMK57 as template, and primers pex34-5 and pex34-6 to amplify *PEX34* deletion cassette, then transformed into *yku80* cells to produce *pex34* deletion strain.

To create *pex34*::Pex32-mGFP, *Bgl*II-linearized pHIPZ-*PEX32*-mGFP was transformed into *pex34* cells. *Xho*I-linearized pSEM01 was integrated into *pex34*::Pex32-mGFP to produce Pex14-mCherry.

Construction of strains expressing *PEX11* under control of the alcohol oxidase promoter (P_{AOX})

Plasmid pHIPH4-*PEX11* was produced by ligation of *Not*I and *Sma*I digested pHIPX4-*PEX11* and pHIPH7-*PEX11*. The plasmid pHIPX4-*PEX11* was constructed as follows: a

PCR fragment containing *PEX11* was obtained using primers Pex11-3 and Pex11-4 with WT genomic DNA as a template. PCR product and pHIPX4 were restricted by *Hin*dIII and *Sal*I, ligated which result in pHIPX4-*PEX11*. pHIPH7-*PEX11* was constructed from the ligation of *Bam*HI and *Xma*I digested pHIPH5-*PEX11* and pHIPH7-DsRed-SKL. To get pHIPH5-*PEX11*, the *PEX11* gene was amplified with primers PEX11-01 and PEX11-02 by using the WT genomic DNA as templates, *Bam*HI and *Xma*I digested PCR fragment was inserted between the *Bam*HI and *Xma*I sites of pSEM04. *Nsi*I-linearized pHIPH4-*PEX11* were integrated into WT::GFP-SKL, *pex11*::GFP-SKL and *pex32*::GFP-SKL strains respectively to produce P_{AOX}Pex11.

Construction of strain expressing Pex34-mGFP under control of the endogenous promoter

A plasmid encoding Pex34-mGFP was constructed as follows: a PCR fragment encoding the C-terminus of Pex34 was obtained using primers pex34 fw and pex34 rev with WT genomic DNA as a template. The obtained PCR fragment was digested with *Bgl*II and *Nru*I, and inserted between the *Bgl*II and *Nru*I sites of plasmid pHIPZ-mGFP fusinator. *Bsm*BI-linearized pHIPZ-*PEX34*-mGFP was transformed into *yku80* cells, producing Pex34-mGFP. *Dra*I-linearized pHIPH7-DsRed-SKL was integrated into Pex34-mGFP to produce DsRed-SKL.

Overproduction of Pex32-mGFP in WT, *pex32*, *pex11* and *pex34* cells

To overproduce Pex32-mGFP, *Aat*II-linearized pHIPN18-*PEX32*-mGFP was integrated into *yku80*::Pmp47-mKate2, *pex11*::Pmp47-mKate2, *pex32*::Pmp47-mKate2 and *pex34* strains separately to produce P_{ADH1}Pex32-mGFP. *Spe*I-linearized pHIPX-*PMP47*-mKate2 was integrated into *yku80*, *pex34*::P_{ADH1}Pex32-mGFP, *pex11*::Pex32-mGFP and *pex34*::Pex32-mGFP separately to produce Pmp47-mKate2.

Preparation of yeast TCA lysates, SDS-PAGE and Western blotting

Cell extracts of TCA-treated cells were prepared for SDS-PAGE as described previously (Baerends et al., 2000). Equal amounts of protein were loaded per lane and blots were probed with anti-mGFP antibodies (sc-9996, Santa Cruz Biotech; 1:2000 dilution), anti-Pex11 antibodies (Knoops et al., 2014; 1:2000 dilution), anti-Pex14 antibodies (Komori et al., 1997; 1:10,000 dilution), anti-Pex3 antibodies (Baerends et al., 1997; 1:5000 dilution), anti-AOX antibodies (van der Klei et al., 1995; 1:10,000 dilution), or anti-pyruvate carboxylase 1 (Pyc1) antibodies (Ozimek et al., 2007; 1:10,000 dilution). Secondary goat anti-rabbit (31460) or goat anti-mouse (31430) antibodies conjugated to horseradish peroxidase (HRP) (Thermo Scientific; 1:5000 dilution) were used for detection. Pyc1 was used as a loading control.

Quantification of Western blots

Blots were scanned using a densitometer (Bio-Rad, GS-710) and protein levels were

quantified using ImageJ software. The intensity of each band measured was normalized by dividing the intensity of the corresponding Pyc1 band (loading control). Normalized values obtained for Pex11, Pex3, Pex14 and AOX levels in WT cells were set to 1 and the levels in *pex32* cells were displayed relative to WT. Standard deviations were calculated using Excel. Significance was determined using two-tailed student's t-test. n.s. represents p-values > 0.05 and *** represents p-values < 0.001. The data presented are derived from three independent experiments.

Fluorescence microscopy

Wide-field FM images were captured at room temperature using a 100×1.30 NA objective (Carl Zeiss, Oberkochen, Germany). Images were acquired using a Zeiss Axioscope A1 fluorescence microscope (Carl Zeiss), Micro-Manager 1.4 software and a CoolSNAP HQ^2 digital camera. The GFP fluorescence were visualized with a 470/40 nm band-pass excitation filter, a 495 nm dichromatic mirror, and a 525/50 nm band-pass emission filter. DsRed fluorescence were visualized with a 546/12 nm band-pass excitation filter, a 560 nm dichromatic mirror, and a 575-640 nm band-pass emission filter. mCherry and mKate2 fluorescence were visualized with a 587/25 nm band-pass excitation filter, a 605 nm dichromatic mirror, and a 670/70 nm band-pass emission filter.

Airy-scan images were captured with a confocal microscope (LSM800; Carl Zeiss) equipped with a 32-channel gallium arsenide phosphide photomultiplier tube (GaAsP-PMT), Zen 2009 software (Carl Zeiss) and a 63x1.40 NA objective (Carl Zeiss, Oberkochen, Germany). The GFP, mKate2 and mCherry fluorescence were visualized with a 488, 561 and 587 nm laser respectively.

Image analysis was performed using ImageJ. Bright field images have been adjusted to only show cell outlines. Figures were prepared using Adobe Illustrator software.

Quantification of peroxisomes numbers

Peroxisomes number quantification for Fig. 2B and Fig. 3B were performed manually based on 200 randomly selected cells from three independent cultures. Similarly, 200 randomly selected cells in two independent experiments were used to manually quantify peroxisomes number for Fig. 8C. Numbers correspond to the average number of peroxisomes per cell or to the average number of cells that do not contain any peroxisomal structures. Standard deviations were calculated using Excel. Significance was determined using two tailed student's t-test. n.s. represents p-values > 0.05 and *** represents p-values < 0.001. For Fig. 6D, peroxisomes were detected and quantified automatically using a custom made plugin (Thomas et al., 2015) from 500 cells of two independent cultures.

Electron microscopy

For morphology analysis, *pex34* cells were fixed in 1.5% potassium permanganate, post-stained with 0.5% uranyl acetate and embedded in Epon (a mixture of Glycid ether

(51.5% w/v; Serva, 151414), Methylnadic anhydride (47.3% w/v; Serva, 140573) and 2,4,6-Tris(dimethylaminomethyl)phenol (1.2% w/v; Santa Cruz, F0112)). Image analysis and distance measurements are performed using ImageJ as described before (Wu et al., 2020).

In *Silico* Analysis

Pex34-related proteins in various yeast species were identified using the primary sequence of *S. cerevisiae* Pex34 in Gapped Blast and Position Specific Iterated (PSI) Blast analyses (Altschul et al., 1997) on the budding yeasts dataset (taxid: 4892) of the non-redundant (nr) protein database at the National Center for Biotechnological Information (NCBI). In the PSI-Blast analyses a statistical significance value of 0.001 was used as a threshold for the inclusion of homologous sequences in each next iteration. Alignments of amino acid sequences were constructed using the Clustal_X2 program (http://www.clustal.org/clustal2/) and displayed using GeneDoc software (Nicholas et al., 1997).

Acknowledgements

The authors thank Rinse de Boer for help discussions and feedbacks on the image analysis.

Funding

This work was supported by a grant from the China Scholarship Council (CSC) to F.W., and from the Nederlandse Organisatie voor Wetenschappelijk Onderzoek/Chemical Sciences (NWO/CW) to A.A. (711.012.002).

References

Altschul, S. F., Madden, T. L., Schäffer, A. A., Zhang, J., Zhang, Z., Miller, W. and Lipman, D. (1997). Gapped BLAST and PSI-BLAST: a new generation of protein database search programs. *Nucleic Acids Res*. **25**, 3389–3402. doi:10.1093/nar/25.17.3389

Baerends, R. J. S., Faber, K. N., Kram, A. M., Kiel, J. A. K. W., van der Klei, I. J. and Veenhuis, M. (2000). A stretch of positively charged amino acids at the N terminals of Hansenula polymorpha Pex3p is involved in incorporation of the protein into the peroxisomal membrane. *J. Biol. Chem.* **275**, 9986–9995. doi:10.1074/jbc.275.14.9986

Baerends, R. J. S., Salomons, F. A., Faber, K. N., Kiel, J. A., van der Klei, I. J. and Veenhuis, M. (1997). Deviant Pex3p levels affect normal peroxisome formation in Hansenula polymorpha: high steady-state levels of the protein fully abolish matrix protein import. Yeast **13**, 1437–1448. doi:10.1002/(SICI)1097-0061(199712)13:15<1437::AID-YEA192>3.0.CO;2-U

Devarajan, S., Meurer, M., van Roermund, C. W. T., Chen, X., Hettema, E. H., Kemp, S., Knop, M. and Williams, C. (2020). Proteasome-dependent protein quality control of the peroxisomal membrane protein Pxa1p. *Biochim. Biophys. Acta Biomembr.* **1862**, 183342. doi:10.1016/j.bbamem.2020.183342

Dulermo, R., Dulermo, T., Gamboa-Meléndez, H., Thevenieau, F. and Nicaud, J. M. (2015). Role of pex11p in lipid homeostasis in Yarrowia lipolytica. *Eukaryot. Cell* **14**, 511–525. doi:10.1128/EC.00051-15

Faber, K. N., Haima, P., Harder, W., Veenhuis, M. and Ab, G. (1994). Highly-efficient electrotransformation of the yeast Hansenula polymorpha. *Curr. Genet.* **25**, 305–310. doi:10.1007/BF00351482

Farré, J. C., Carolino, K., Stasyk, O. V., Stasyk, O. G., Hodzic, Z., Agrawal, G., Till, A., Proietto, M., Cregg, J., Sibirny, A. A. and Subramani, S. (2017). A New Yeast Peroxin, Pex36, a Functional Homolog of Mammalian PEX16, Functions in the ER-to-Peroxisome Traffic of Peroxisomal Membrane Proteins. *J. Mol. Biol.* **429**, 3743–3762. doi:10.1016/j.jmb.2017.10.009

Farré, J., Mahalingam, S. S., Proietto, M. and Subramani, S. (2019). Peroxisome biogenesis, membrane contact sites, and quality control. *EMBO Rep.* **20**, e46864. doi:10.15252/embr.201846864

Gietl, C., Faber, K. N., van der Klei, I. J. and Veenhuis, M. (1994). Mutational analysis of the N-terminal topogenic signal of watermelon glyoxysomal malate dehydrogenase using the heterologous host Hansenula polymorpha. *Proc. Natl. Acad. Sci. USA* **91**, 3151–3155. doi:10.1073/pnas.91.8.3151

He, W., Shi, Q., Hu, X. and Yan, R. (2007). The membrane topology of RTN3 and its effect on binding of RTN3 to BACE1. *J. Biol. Chem.* **282**, 29144–29151. doi:10.1074/jbc.M704181200

Joshi, A. S., Huang, X., Choudhary, V., Levine, T. P., Hu, J. and Prinz, W. A. (2016). A family of membrane-shaping proteins at ER subdomains regulates pre-peroxisomal vesicle biogenesis. *J. Cell Biol.* **215**, 515–529. doi:10.1083/jcb.201602064

Knoops, K., Manivannan, S., Cepińska, M. N., Krikken, A. M., Kram, A. M., Veenhuis, M. and van der Klei, I. J. (2014). Preperoxisomal vesicles can form in the absence of Pex3. *J. Cell Biol.* **204**, 659–668. doi:10.1083/jcb.201310148

Komduur, J. A., Veenhuis, M. and Kiel, J. A. K. W. (2003). The Hansenula polymorpha PDD7 gene is essential for macropexophagy and microautophagy. *FEMS Yeast Res.* **3**, 27–34. doi:10.1016/S1567-1356(02)00135-6

Komori, M., Rasmussen, S. W., Kiel, J. A. K. W., Baerends, R. J. S., Cregg, J. M., Van Der Klei, I. J. and Veenhuis, M. (1997). The Hansenula polymorpha PEX14 gene encodes a novel peroxisomal membrane protein essential for peroxisome biogenesis. *EMBO J. 16*(1), 44–53. doi:10.1093/emboj/16.1.44

Kopec, K. O., Alva, V. and Lupas, A. N. (2010). Homology of SMP domains to the TULIP superfamily of lipid-binding proteins provides a structural basis for lipid exchange between ER and mitochondria. *Bioinformatics* **26**, 1927–1931. doi:10.1093/bioinformatics/btq326

Krikken, A. M., Veenhuis, M. and van der Klei, I. J. (2009). Hansenula polymorpha pex11 cells are affected in peroxisome retention. *FEBS J*. **276**, 1429–1439. doi:10.1111/j.1742-4658.2009.06883.x

Krikken, A. M., Wu, H., de Boer, R., Devos, D. P., Levine, T. P. and van der Klei, I. J. (2020). Peroxisome retention involves Inp1-dependent peroxisome-plasma membrane contact sites in yeast. *J. Cell Biol*. **219**. doi:10.1083/jcb.201906023

Lee, M., Moon, Y., Lee, S., Lee, C. and Jun, Y. (2019). Ergosterol interacts with Sey1p to promote atlastin-mediated endoplasmic reticulum membrane fusion in Saccharomyces cerevisiae. *FASEB J*. **33**, 3590–3600. doi:10.1096/fj.201800779RR

Mattiazzi Ušaj, M., Brložnik, M., Kaferle, P., Žitnik, M., Wolinski, H., Leitner, F., Kohlwein, S. D., Zupan, B. and Petrovič, U. (2015). Genome-wide localization study of yeast pex11 identifies peroxisome-mitochondria interactions through the ERMES complex. *J. Mol. Biol*. **427**, 2072-2087. doi:10.1016/j.jmb.2015.03.004

Ozimek, P. Z., Klompmaker, S. H., Visser, N., Veenhuis, M. and van der Klei, I. J. (2007). The transcarboxylase domain of pyruvate carboxylase is essential for assembly of the peroxisomal flavoenzyme alcohol oxidase. *FEMS Yeast Res*. **7**, 1082–1092. doi:10.1111/j.1567-1364.2007.00214.x

Saraya, R., Cepińska, M. N., Kiel, J. A. K. W., Veenhuis, M. and van der Klei, I. J. (2010). A conserved function for Inp2 in peroxisome inheritance. *Biochim. Biophys. Acta* **1803**, 617–622. doi:10.1016/j.bbamcr.2010.02.001

Saraya, R., Krikken, A. M., Kiel, J. A. K. W., Baerends, R. J. S., Veenhuis, M. and van der Klei, I. J. (2012). Novel genetic tools for Hansenula polymorpha. *FEMS Yeast Res*. **12**, 271–278. doi:10.1111/j.1567-1364.2011.00772.x

Shai, N., Yifrach, E., Van Roermund, C. W. T., Cohen, N., Bibi, C., Ijlst, L., Cavellini, L., Meurisse, J., Schuster, R., Zada, L., et al., (2018). Systematic mapping of contact sites reveals tethers and a function for the peroxisome-mitochondria contact. *Nat. Commun*. **9**, 1761. doi:10.1038/s41467-018-03957-8

Smith, J. J. and Aitchison, J. D. (2013). Peroxisomes take shape. *Nat. Rev. Mol. Cell Biol*. **14**, 803–817. doi:10.1038/nrm3700

Sudbery, P. E., Gleeson, M. A., Veale, R. A., Ledeboer, A. M. and Zoetmulder, M. C. (1988). Hansenula polymorpha as a novel yeast system for the expression of heterologous genes. *Biochem. Soc. Trans*. **16**, 1081-1083. doi:10.1042/bst0161081a

Thomas, A. S., Krikken, A. M., de Boer, R. and Williams, C. (2018). Hansenula polymorpha Aat2p is targeted to peroxisomes via a novel Pex20p-dependent pathway. *FEBS Lett*. **592**, 2466–2475. doi:10.1002/1873-3468.13168

Tower, R. J., Fagarasanu, A., Aitchison, J. D. and Rachubinski, R. A. (2011). The peroxin Pex34p functions with the Pex11 family of peroxisomal divisional proteins to regulate the peroxisome population in yeast. *Mol. Biol. Cell 22*(10), 1727–1738. doi:10.1091/mbc.E11-01-0084

van der Klei, I. J., Hilbrands, R. E., Swaving, G. J., Waterham, H. R., Vrieling, E. G., Titorenko, V. I., Cregg, J. M., Harder, W. and Veenhuis, M. (1995). The Hansenula polymorpha PER3 gene is essential for the import of PTS1 proteins into the peroxisomal matrix. *J. Biol. Chem*. **270**, 17229–17236. doi:10.1074/jbc.270.29.17229

Van Dijken, L. P., Otto, R. and Harder, W. (1976). Growth of Hansenula polymorpha in a methanol-limited chemostat. *Arch. Microbiol*. **111**, 137–144. doi:10.1007/BF00446560

Wu, F., de Boer, R., Krikken, A. M., Akşit, A., Bordin, N., Devos, D. P. and van der Klei, I. J. (2020). Pex24 and Pex32 are required to tether peroxisomes to the ER for organelle biogenesis, positioning and segregation in yeast. *J*. *Cell Sci*. **133**. doi:10.1242/jcs.246983

Wu, H., de Boer, R., Krikken, A. M., Akşit, A., Yuan, W. and van der Klei, I. J. (2018). Peroxisome development in yeast is associated with the formation of Pex3-dependent peroxisome-vacuole contact sites. *Biochim*. *Biophys*. *Acta Mol*. *Cell Res*. **1868**, 349–359. doi:10.1016/j.bbamcr.2018.08.021

Yamamoto, Y. and Sakisaka, T. (2018). The peroxisome biogenesis factors posttranslationally target reticulon homology domain-containing proteins to the endoplasmic reticulum membrane. *Sci*. *Rep*. **8**, 2322. doi:10.1038/s41598-018-20797-0

Yan, M., Rachubinski, D. A., Joshi, S., Rachubinski, R. A. and Subramani, S. (2008). Dysferlin Domain-containing Proteins, Pex30p and Pex31p, Localized to Two Compartments, Control the Number and Size of Oleate-induced Peroxisomes in Pichia pastoris. *Mol*. *Biol*. *Cell* **19**, 885–898. doi:10.1091/mbc.e07-10-1042

Yan, R., Shi, Q., Hu, X. and Zhou, X. (2006). Reticulon proteins: Emerging players in neurodegenerative diseases. *Cell*. *Mol*. *Life Sci*. **63**, 877–889. doi:10.1007/s00018-005-5338-2

Yuan, W., Veenhuis, M. and van der Klei, I. J. (2016). The birth of yeast peroxisomes. *Biochim*. *Biophys*. *Acta Mol*. *Cell Res*. **1863**, 902–910. doi:10.1016/j.bbamcr.2015.09.008

Table 1. Strains used in this study

Strain	Description	Reference
WT	NCYC495; *leu 1.1*	(Sudbery et al., 1988)
WT:: *yku80*	NCYC495 *yku80* deletion strain; *leu 1.1*, *URA3*	(Saraya et al., 2012)
pex32	*yku80* with *PEX32* deletion strain; *leu 1.1*, *URA3*, Zeo^R	(Wu et al., 2020)
Pex32-mGFP	*yku80* with pHIPZ-*PEX32*-mGFP; *leu 1.1*, *URA3*, Zeo^R	(Wu et al., 2020)
pex32::P$_{ADH1}$Pex32-mGFP	*pex32* with pHIPN18-*PEX32*-mGFP; *leu 1.1*, *URA3*, Zeo^R, Nat^R	This study
pex32::P$_{ADH1}$Pex32$^{TM(I-IV)}$-mGFP	*pex32* with pHIPN18-*PEX32*$^{TM(I-IV)}$-mGFP; *leu 1.1*, *URA3*, Zeo^R, Nat^R	This study
pex32::P$_{ADH1}$Pex32$^{TM(I-III)}$-mGFP	*pex32* with pHIPN18-*PEX32*$^{TM(I-III)}$-mGFP; *leu 1.1*, *URA3*, Zeo^R, Nat^R	This study
pex32::P$_{ADH1}$Pex32$^{TM(I-II)}$-mGFP	*pex32* with pHIPN18-*PEX32*$^{TM(I-II)}$-mGFP; *leu 1.1*, *URA3*, Zeo^R, Nat^R	This study
pex32::P$_{ADH1}$Pex32$^{TM(I)}$-mGFP	*pex32* with pHIPN18-*PEX32*$^{TM(I)}$-mGFP; *leu 1.1*, *URA3*, Zeo^R, Nat^R	This study
pex32::P$_{ADH1}$Pex32$^{TM(II-IV)}$-mGFP	*pex32* with pHIPN18-*PEX32*$^{TM(II-IV)}$-mGFP; *leu 1.1*, *URA3*, Zeo^R, Nat^R	This study
pex32::P$_{ADH1}$Pex32$^{\Delta 31}$-mGFP	*pex32* with PHIPN18-*PEX32*$^{\Delta 31}$-mGFP; *leu 1.1*, *URA3*, Zeo^R, Nat^R	This study
pex32::P$_{ADH1}$Pex32^{DysF}-mGFP	*pex32* with PHIPN18-*PEX32*^{DysF}-mGFP; *leu 1.1*, *URA3*, Zeo^R, Nat^R	This study
pex32::BiP-mCherry-HDEL	*pex32* with pHIPX7-BiP$_{N30}$-mCherry-HDEL; *URA3*, Zeo^R, *LEU2*	This study
pex32::P$_{ADH1}$Pex32-mGFP::BiP-mCherry-HDEL	*pex32*::P$_{ADH1}$Pex32-mGFP with pHIPX7-BiP$_{N30}$-mCherry-HDEL; *URA3*, Zeo^R, Nat^R, *LEU2*	This study
pex32::P$_{ADH1}$Pex32$^{TM(I-IV)}$-mGFP::BiP-mCherry-HDEL	*pex32*::P$_{ADH1}$Pex32$^{TM(I-IV)}$-mGFP with pHIPX7-BiP$_{N30}$-mCherry-HDEL; *URA3*, Zeo^R, Nat^R, *LEU2*	This study
pex32::P$_{ADH1}$Pex32$^{TM(I-III)}$-mGFP::Bip-mCherry-HDEL	*pex32*::P$_{ADH1}$Pex32$^{TM(I-III)}$-mGFP with pHIPX7-BiP$_{N30}$-mCherry-HDEL; *URA3*, Zeo^R, Nat^R, *LEU2*	This study
pex32::P$_{ADH1}$Pex32$^{TM(I-II)}$-mGFP::BiP-mCherry-HDEL	*pex32*::P$_{ADH1}$Pex32$^{TM(I-II)}$-mGFP with pHIPX7-BiP$_{N30}$-mCherry-HDEL; *URA3*, Zeo^R, Nat^R, *LEU2*	This study
pex32::P$_{ADH1}$Pex32$^{TM(I)}$-mGFP::BiP-mCherry-HDEL	*pex32*::P$_{ADH1}$Pex32$^{TM(I)}$-mGFP with pHIPX7-BiP$_{N30}$-mCherry-HDEL; *URA3*, Zeo^R, Nat^R, *LEU2*	This study
pex32::P$_{ADH1}$Pex32$^{TM(II-IV)}$-mGFP::BiP-mCherry-HDEL	*pex32*::P$_{ADH1}$Pex32$^{TM(II-IV)}$-mGFP with pHIPX7-BiP$_{N30}$-mCherry-HDEL; *URA3*, Zeo^R, Nat^R, *LEU2*	This study
pex32::P$_{ADH1}$Pex32$^{\Delta 31}$-mGFP::BiP-mCherry-HDEL	*pex32*::P$_{ADH1}$Pex32$^{\Delta 31}$-mGFP with pHIPX7-BiP$_{N30}$-mCherry-HDEL; *URA3*, Zeo^R, Nat^R, *LEU2*	This study
pex32::P$_{ADH1}$Pex32^{DysF}-mGFP::BiP-mCherry-HDEL	*pex32*::P$_{ADH1}$Pex32^{DysF}-mGFP with pHIPX7-BiP$_{N30}$-mCherry-HDEL; *URA3*, Zeo^R, Nat^R, *LEU2*	This study
pex32::P$_{ADH1}$Pex32$^{TM(II)}$-mGFP::BiP-mCherry-HDEL	*pex32::BiP-mCherry-HDEL* with pHIPN18-*PEX32*$^{TM(II)}$-mGFP; *URA3*, Zeo^R, *LEU2*, Nat^R	This study
pex32::P$_{ADH1}$Pex32$^{TM(III-IV)}$-mGFP::BiP-mCherry-HDEL	*pex32::BiP-mCherry-HDEL* with pHIPN18-*PEX32*$^{TM(III-IV)}$-mGFP; *URA3*, Zeo^R, *LEU2*, Nat^R	This study
pex32::Pmp47-mKate2	*pex32* with pHIPX-*PMP47*-mKate2*; URA3*, Zeo^R, *LEU2*	This study
Pex32^{FL}-mGFP::Pmp47-mKate2	Pex32-mGFP with pHIPX-*PMP47*-mKate2*; URA3*, Zeo^R, *LEU2*	This study

Strain	Description	Reference
pex32::Pex32$^{TM(I-IV)}$-mGFP::Pmp47-mKate2	*pex32*::Pmp47-mKate2 with pHIPN22-*PEX32*$^{TM(I-IV)}$-mGFP; *URA3*, Zeo^R, *LEU2*, Nat^R	This study
pex32::Pex32$^{TM(I-III)}$-mGFP::Pmp47-mKate2	*pex32*::Pmp47-mKate2 with pHIPN22-*PEX32*$^{TM(I-III)}$-mGFP; *URA3*, Zeo^R, *LEU2*, Nat^R	This study
pex32::Pex32$^{TM(I-II)}$-mGFP::Pmp47-mKate2	*pex32*::Pmp47-mKate2 with pHIPN22-*PEX32*$^{TM(I-II)}$-mGFP; *URA3*, Zeo^R, *LEU2*, Nat^R	This study
pex32::Pex32$^{TM(I)}$-mGFP::Pmp47-mKate2	*pex32*::Pmp47-mKate2 with pHIPN22-*PEX32*$^{TM(I)}$-mGFP; *URA3*, Zeo^R, *LEU2*, Nat^R	This study
pex32::Pex32$^{TM(II-IV)}$-mGFP::Pmp47-mKate2	*pex32*::Pmp47-mKate2 with pHIPN22-*PEX32*$^{TM(II-IV)}$-mGFP; *URA3*, Zeo^R, *LEU2*, Nat^R	This study
pex32::Pex32$^{\Delta 31}$-mGFP::Pmp47-mKate2	*pex32*::Pmp47-mKate2 with pHIPN22-*PEX32*$^{\Delta 31}$-mGFP; *URA3*, Zeo^R, *LEU2*, Nat^R	This study
pex32::Pex32^{DysF}-mGFP::Pmp47-mKate2	*pex32*::Pmp47-mKate2 with pHIPN22-*PEX32*^{DysF}-mGFP; *URA3*, Zeo^R, *LEU2*, Nat^R	This study
pex32 atg1	*pex32* with *ATG1* deletion cassette; *leu 1.1*, *URA3*, Zeo^R, Hph^R	This study
pex32 atg1::DsRed-SKL	*pex32 atg1* with pAMK15; *URA3*, Zeo^R, Hph^R, *LEU2*	This study
WT::DsRed-SKL	*yku80* with pHIPN18-DsRed-SKL; *leu 1.1*, *URA3*, Nat^R	(Wu et al., 2020)
pex32::DsRed-SKL	*pex32* with pAMK15; *URA3*, Zeo^R, *LEU2*	(Wu et al., 2020)
pex11	*PEX11* deletion strain; *leu 1.1*, *URA3*	(Krikken et al., 2009)
pex3	*PEX3* deletion strain; *leu 1.1*, *URA3*	(Baerends et al., 1997)
pex14	*PEX14* deletion strain; *leu 1.1*, *URA3*	(Komori et al., 1997)
WT::GFP-SKL	*yku80* with pFEM35; *URA3*, *LEU2*	(Krikken et al., 2009)
WT::GFP-SKL::P_{AOX}Pex11	WT::GFP-SKL with pHIPH4-*PEX11*; *URA3*, *LEU2*, Hph^R	This study
pex11::GFP-SKL	*pex11* with pFEM35; *URA3*, *LEU2*	(Krikken et al., 2009)
pex11::GFP-SKL::P_{AOX}Pex11	*pex11*::GFP-SKL with pHIPH4-*PEX11*; *URA3*, *LEU2*, Hph^R	This study
pex32::GFP-SKL	*pex32* with pFEM35; *URA3*, Zeo^R, *LEU2*	(Wu et al., 2020)
pex32::GFP-SKL::P_{AOX}Pex11	*pex32*::GFP-SKL with pHIPH4-*PEX11*; *URA3*, *LEU2*, Hph^R	This study
pex34	*yku80* with *PEX34* deletion strain; *leu 1.1*, *URA3*, Hph^R	This study
pex34::Pex32-mGFP	*pex34* with pHIPZ-*PEX32*-mGFP; *leu 1.1*, *URA3*, Hph^R, Zeo^R	This study
pex34::Pex32-mGFP::Pex14-mCherry	*pex34*::Pex32-mGFP with pSEM01; *leu 1.1*, *URA3*, Hph^R, Zeo^R, Nat^R	This study
Pex34-mGFP	*yku80* with pHIPZ-*PEX34*-mGFP; *leu 1.1*, URA3, Zeo^R	This study
Pex34-mGFP::DsRed-SKL	Pex34-mGFP with pHIPH7-DsRed-SKL; *leu 1.1*, *URA3*, Zeo^R, Hph^R	This study
Pmp47-mKate2	*yku80* with pHIPX-*PMP47*-mKate2; *URA3*, *LEU2*	This study
WT::Pmp47-mKate2::P_{ADH1}Pex32-GFP	Pmp47-mKate2 with pHIPN18-*PEX32*-GFP; *URA3*, *LEU2*, Nat^R	This study
pex11::Pmp47-mKate2	*pex11* with pHIPX-*PMP47*-mKate2; *URA3*, *LEU2*	This study
pex11::Pmp47-mKate2::P_{ADH1}Pex32-GFP	*pex11*::Pmp47-mKate2 with pHIPN18-*PEX32*-GFP; *URA3*, *LEU2*, Nat^R	This study

Strain	Description	Reference
pex34::P_{ADH1}Pex32-GFP	*pex34* with pHIPN18-*PEX32*-GFP; *leu1.1*, *URA3*, Hph^R, Nat^R	This study
pex34::Pmp47-mKate2::P_{ADH1}Pex32-GFP	*pex34*::P_{ADH1}Pex32-GFP with pHIPX-*PMP47*-mKate2; *URA3*, Hph^R, Nat^R, *LEU2*	This study
pex32::Pmp47-mKate2::P_{ADH1}Pex32-GFP	*pex32*::Pmp47-mKate2 with pHIPN18-*PEX32*-GFP; *URA3*, Zeo^R, *LEU2*, Nat^R	This study
pex11::Pex32-mGFP	*pex11* with pHIPZ-*PEX32*-mGFP; *leu 1.1*, *URA3*, Zeo^R	(Wu et al. 2020)
pex11::Pex32-mGFP::Pmp47-mKate2	*pex11*::Pex32-GFP with pHIPX-*PMP47*-mKate2; *URA3*, Zeo^R, *LEU2*	This study
pex34::Pex32-mGFP::Pmp47-mKate2	*pex34*::Pex32-GFP with pHIPX-*PMP47*-mKate2; *URA3*, Hph^R, Zeo^R, *LEU2*	This study

Table 2. Plasmids used in this study

Plasmid	Description	Reference
pHIPZ18-*INP1*-GFP	pHIPZ plasmid containing the full length of *INP1* fused with mGFP under the control of *ADH1* promoter; Zeo^R, Amp^R	(Krikken et al., 2020)
pHIPZ18-*PEX32*$^{TM(I-IV)}$-mGFP	pHIPZ plasmid containing *PEX32*$^{TM(I-IV)}$ fused with mGFP under the control of *ADH1* promoter; Zeo^R, Amp^R	This study
pHIPZ18-*PEX32*^{DysF}-mGFP	pHIPZ plasmid containing *PEX32*^{DysF} fused with mGFP under the control of *ADH1* promoter; Zeo^R, Amp^R	This study
pAMK106	pHIPN plasmid containing eGFP-SKL under the control of *ADH1* promoter; Nat^R, Amp^R	(Krikken et al., 2020)
pHIPN18-Pex32$^{TM(I-IV)}$-mGFP	pHIPN plasmid containing *PEX32*$^{TM(I-IV)}$ fused with mGFP under the control of *ADH1* promoter; Nat^R, Amp^R	This study
pHIPN18-*Pex32*^{DysF}-mGFP	pHIPN plasmid containing *PEX32*^{DysF} fused with mGFP under the control of *ADH1* promoter; Nat^R, Amp^R	This study
pHIPN18-*PEX32*$^{TM(I-III)}$-mGFP	pHIPN plasmid containing *PEX32*$^{TM(I-III)}$ fused with mGFP under the control of *ADH1* promoter; Nat^R, Amp^R	This study
pHIPN18-*PEX32*$^{TM(I-II)}$-mGFP	pHIPN plasmid containing *PEX32*$^{TM(I-II)}$ fused with mGFP under the control of *ADH1* promoter; Nat^R, Amp^R	This study
pHIPN18-*PEX32*$^{TM(I)}$-mGFP	pHIPN plasmid containing *PEX32*$^{TM(I)}$ fused with mGFP under the control of *ADH1* promoter; Nat^R, Amp^R	This study
pHIPN18-*PEX32*$^{TM(II-IV)}$-mGFP	pHIPN plasmid containing *PEX32*$^{TM(II-IV)}$ fused with mGFP under the control of *ADH1* promoter; Nat^R, Amp^R	This study
pHIPN18-*PEX32*$^{\Delta 31}$-mGFP	pHIPN plasmid containing *PEX32*$^{\Delta 31}$ fused with mGFP under the control of *ADH1* promoter; Nat^R, Amp^R	This study
pHIPN18-*PEX32*-mGFP	pHIPN plasmid containing the full length of *PEX32* fused with GFP under the control of *ADH1* promoter; Nat^R, Amp^R	This study
pHIPX7-BiP_{N30}-mCherry-HDEL	pHIPX plasmid containing BiP_{N30} fused to mCherry-HDEL under control of *TEF* promoter; *LEU2*, Kan^R	(Wu et al., 2020)
pHIPX-*PMP47*-mKate2	pHIPX plasmid containing the C-terminal region of *PMP47* fused with mKate2; *LEU2,* Amp^R	(Krikken et al., 2020)
pHIPN18-*PEX32*$^{TM(II)}$-mGFP	pHIPN plasmid containing *PEX32*$^{TM(II)}$ fused with mGFP under the control of *ADH1* promoter; Nat^R, Amp^R	This study
pHIPN18-*PEX32*$^{TM(III-IV)}$-mGFP	pHIPN plasmid containing *PEX32*$^{TM(III-IV)}$ fused with mGFP under the control of *ADH1* promoter; Nat^R, Amp^R	This study
pHIPN22-*PEX32*$^{TM(I-IV)}$-mGFP	pHIPN plasmid containing *PEX32*$^{TM(I-IV)}$ fused with mGFP under the control of *PEX32* promoter; Nat^R, Amp^R	This study
pHIPN22-*PEX32*$^{TM(I-III)}$-mGFP	pHIPN plasmid containing *PEX32*$^{TM(I-III)}$ fused with mGFP under the control of *PEX32* promoter; Nat^R, Amp^R	This study
pHIPN22-*PEX32*$^{TM(I-II)}$-mGFP	pHIPN plasmid containing *PEX32*$^{TM(I-II)}$ fused with mGFP under the control of *PEX32* promoter; Nat^R, Amp^R	This study
pHIPN22-*PEX32*$^{TM(I)}$-mGFP	pHIPN plasmid containing *PEX32*$^{TM(I)}$ fused with mGFP under the control of *PEX32* promoter; Nat^R, Amp^R	This study
pHIPN22-*PEX32*$^{TM(II-IV)}$-mGFP	pHIPN plasmid containing *PEX32*$^{TM(II-IV)}$ fused with mGFP under the control of *PEX32* promoter; Nat^R, Amp^R	This study
pHIPN22-*PEX32*$^{\Delta 31}$-mGFP	pHIPN plasmid containing *PEX32*$^{\Delta 31}$ fused with mGFP under the control of *PEX32* promoter; Nat^R, Amp^R	This study

Plasmid	Description	Reference
pHIPN22-*PEX32*^{DysF}-mGFP	pHIPN plasmid containing *PEX32*^{DysF} fused with mGFP under the control of *PEX32* promoter; Nat^R, Amp^R	This study
pARM011	Plasmid containing the *ATG1* deletion cassette; Hph^R, Amp^R	(Thomas et al., 2018)
pAMK15	pHIPX plasmid containing DsRed-SKL under the control of *TEF* promoter; *LEU2*, Kan^R	(Krikken et al., 2009)
pHIPH4 *PEX11*	pHIPH plasmid containing the full length of *PEX11* under the control of *AOX* promoter; Hph^R, Amp^R	This study
pHIPX4 *PEX11*	pHIPX plasmid containing the full length of *PEX11* under the control of *AOX* promoter; *LEU2*, Kan^R	This study
pHIPX4	pHIPX plasmid with *AOX* promoter; *LEU2*, Kan^R	(Gietl et al., 1994)
pHIPH7 *PEX11*	pHIPH plasmid containing the full length of *PEX11* under the control of *TEF* promoter; Hph^R, Amp^R	This study
pHIPH5-*PEX11*	pHIPH plasmid containing the full length of *PEX11* under the control of *AMO* promoter; Hph^R, Amp^R	This study
pHIPH7-DsRed-SKL	pHIPH plasmid containing DsRed-SKL under the control of *TEF* promoter; Hph^R, Amp^R	(Devarajan et al., 2020)
pSEM04	pHIPH plasmid containing *PEX3* under the control of *AMO* promoter; Hph^R, Amp^R	(Knoops et al., 2014)
pDONR P4-P1R	Multisite Gateway vector; Kan^R, Cm^R	Invitrogen
pDONR P2R-P3	Multisite Gateway vector; Kan^R, Cm^R	Invitrogen
pENTR *PEX34* 5'	pDONR P4-P1R with 5' flanking region of *PEX34*; Kan^R	This study
pENTR *PEX34* 3'	pDONR P2R-P3 with 3' flanking region of *PEX34*; Kan^R	This study
pENTR221-hph	pDONR221 with *HPH* marker; Hph^R, Kan^R	(Saraya et al., 2012)
pDEST-R4-R3	Multisite Gateway donor vector; Amp^R, Cm^R	Invitrogen
pAMK57	Plasmid containing *PEX34* deletion cassette; Hph^R, Amp^R	This study
pHIPZ-*PEX32*-mGFP	pHIPZ plasmid containing the C-terminal region of *PEX32* fused with mGFP; Zeo^R, Amp^R	(Wu et al., 2020)
pSEM01	pHIPN plasmid containing C-terminalregion of *PEX14* fused with mCherry; Nat^R, Amp^R	(Knoops et al., 2014)
pAMK58	pHIPZ plasmid containing gene encoding C-terminal of Pex34 fused to mGFP; Zeo^R, Amp^R	This study
pHIPZ-mGFP	pHIPZ plasmid containing mGFP; Zeo^R, Amp^R	(Saraya et al., 2010)

Table 3. Primers used in this study

Primer	Sequences (5' to 3')
Fw $Pex32_{1-696}$	GCGAAGCTTATGTCTGAGCCCAATGTTCG
Rv $Pex32_{1-696}$	GGAAGATCTGATCTGGAAATCATTGAGCAC
Fw $Pex32_{697-1062}$	GCGAAGCTTATGTCAAATATTGGAACAGG
Rv $Pex32_{697-1062}$	GGAAGATCTGGTGGTTGCGTCGTCCTCG
Rev $Pex32_{1-501}$	GGAAGATCTTCGCGTCATGAGCCAAATG
Rev $Pex32_{1-312}$	GGAAGATCTGTCAATGGTGGTCTTCAAG
Rev $Pex32_{1-177}$	GGAAGATCTAGGATCATCGTTTGTCCAGG
Fw $Pex32_{(169-1062)}$	GCGAAGCTTATGGATGATCCTTATACC
Fw $Pex32_{(94-1062)}$	GCGAAGCTTATGACATCTGCACTGTATGCG
Rv $DysF_{PEX32\text{-}mGFP}$	CCGCTCGAGTTACTTGTACAGCTCGTCCATGCC
Fw $Pex32_{o2TM}$	GCGAAGCTTATGGATGATCCTTATACCA
Fw $Pex32_{TM3+4}$	GCGAAGCTTATGGACTTGCGGTCGGAGAC
P_{PEX32} fw	GAATGCGGCCGCCTCGTGGATGTCTTGATAAC
P_{PEX32} rev	CCCAAGCTTAAGAAGAGGTCATAAATGGAG
pDEL_ATG1_fwd	ACAGGTCGTTGGTGACTTTAC
pDEL_ATG1_rev	CTTCTCGTTGCCCGTGACC
Pex11-3	CCCAAGCTTATGGTTTGCGACACGATAAC
Pex11-4	AGAGTCGACTCATAGCACAGAAGACTCGG
PEX11-01	TCGAGGATCCATGGTTTGCGACACGATAAC
PEX11-02	CGATCCCGGGTCATAGCACAGAAGACTCGG
pex34-1	GGGGACAACTTTGTATAGAAAAGTTGCGGCAGAGTTGGCTGTTCCTTC
pex34-2	GGGGACTGCTTTTTTGTACAAACTTGGTAGAGCTTCTGCGTCGTTGT
pex34-3	GGGGACAGCTTTCTTGTACAAAGTGGAACGAGCTGGTTCTGGATCTGA
pex34-4	GGGGACAACTTTGTATAATAAAGTTGGAGAAGACTACCGACGAGGTT
pex34-5	GCAGAGTTGGCTGTTCCTTC
pex34-6	CTACCGACGAGGTTTTCGGT
pex34 fw	CAGCAGTCCTACGCTCTATT
pex34 rev	AGAAGATCTTAAATACTGTTTCTGCATAG

3